JOURNAL OF GUIDANCE, CONTROL, AND DYNAMICS
Vol. 21, No. 4, July–August 1998

Multibody Effect on Nutational Dynamics of Spin-Stabilized Satellites with Fuel Sloshing

Takashi Nagata*
Kyushu Institute of Technology, Kitakyushu, Fukuoka 804-8550, Japan
Vinod J. Modi†
University of British Columbia, Vancouver, British Columbia V6T 1Z4, Canada
and
Hiroki Matsuo‡
Institute of Space and Astronautical Science, Sagamihara, Kanagawa 229, Japan

A simple and direct approach is presented to study nutational dynamics of spin-stabilized spacecraft with liquid fuel sloshing. It focuses on the effect of multibody interaction between the liquid and the satellite on the nutation time constant, aiming at extrapolation of the ground-test data to on-orbit systems. The system is modeled as a rigid-multibody system, and the liquid friction is introduced as a generalized force. The liquid has finite inertia and three degrees of freedom representing longitudinal and lateral sloshes, as well as circulatory motion about its axis. Ground-based experiments were also carried out, and nutation time constants of a gas-bearing-supported satellite model in several configurations were measured. The liquid friction parameters are evaluated both experimentally and theoretically. Comparison of these values shows that, in general, the plate flow theory tends to overestimate the liquid friction parameters. The experimental results are in rather good correspondence with the estimated values based on the simulation. The numerical study also indicates that ground-based experiments can underestimate the nutation time constants of systems in space.

Nomenclature

$[\boldsymbol{a}\times]$ = matrix equivalent to the vector product operation $\boldsymbol{a}\times$; Eq. (4)
C_a, N_a = liquid friction parameters for agitation; Eq. (7)
C_a^*, N_a^* = nondimensional liquid friction parameters for agitation; Eq. (12b)
C_s, N_s = liquid friction parameters for sloshing; Eq. (7)
C_s^*, N_s^* = nondimensional liquid friction parameters for sloshing; Eq. (12b)
f_L = liquid friction force with reference to the L-frame; Eq. (9a)
T_{nut} = nutation time constant; Eq. (18)
V_a, V_s = velocities of agitation and sloshing, respectively; Eq. (6b)
$\boldsymbol{v}_a$, $\boldsymbol{v}_s$ = vectors representing the directions of agitation and sloshing, respectively; Eq. (6b)
θ_{nut} = nutation angle; Eq. (17)
$\boldsymbol{\tau}_L$ = liquid friction torque with respect to the L-frame; Eq. (9b)
$\boldsymbol{\omega}_a$, $\boldsymbol{\omega}_s$ = agitation and sloshing angular velocities, respectively; Eq. (5)
ω_{sp} = spin rate

I. Introduction

THE Institute of Space and Astronautical Science (ISAS) has launched several scientific satellites using the M-3SII rockets, which consist of three stages of solid rocket motors. For a spin-stabilized satellite, the third-stage motor with the payload (satellite) is spun up to a desired angular velocity before injection. One of the critical issues is the attitude dynamics, which affects accuracy of the resulting trajectory. The nutation divergence caused by energy dissipation due to sloshing of liquid fuel in the satellites is of particular concern. Aiming at more precise estimate of the nutation divergence, basic ground experiments have been carried out by ISAS using a gas-bearing-supported satellite model in several configurations.

Although many papers dealing with dynamics of fluid in coaxially located rotating containers or tanks without spin under uniform gravity have been published,[1–4] there is relatively little literature on vibration modes of liquid partially filled in spinning off-axis tanks. The approach by El-Raheb and Wagner[5] based on a homogeneous vortex assumption was not very successful. Slafer and Challoner[6] investigated interaction between the payload control system and the liquid propellant on dual-spin spacecraft by deriving the closed-loop transfer function using linearized equations of motion incorporated with an empirical liquid model. The authors pointed out that the two-degree-of-freedom pendulum model for liquid dynamics is inaccurate, sometimes resulting in unstable attitude control designs. Agrawal[7] developed a boundary-layer model for analyzing dynamic characteristics of liquid motion in partially filled tanks of a spinning spacecraft. It is based on an analytical solution of the boundary-layer equations in conjunction with finite element analyses of the inviscid and viscous parts of the problem. The author suggested the existence of significant circulatory motion due to the Coriolis forces. However, the nutation time constants obtained by the elaborate model compared with the experimental data rather qualitatively, and the error was up to one order of magnitude for some inertia ratios. Hence, under the present situation, it is more realistic to establish extrapolation of the time constant measured in ground tests, rather than attempt complete analytical prediction.

With this as background, this paper presents a simple and direct approach to study nutational dynamics of spinning spacecraft. It focuses on the effect of multibody interaction between the liquid and the satellite on the nutation time constant. The system is modeled as a rigid-multibody system, and the liquid friction is introduced as a generalized force. Noting the failure of the two-degree-of-freedom model,[6] longitudinal and lateral sloshes, as well as circulatory motion of the liquid about its axis of symmetry (agitation), are taken into account. The liquid friction parameters are evaluated both experimentally and theoretically. A comparison of the numerical and

Received April 3, 1997; revision received Jan. 11, 1998; accepted for publication Jan. 29, 1998.

*Lecturer, Department of Mechanical Engineering, 1-1 Sensuicho, Tobata. Member AIAA.
†Professor Emeritus, Department of Mechanical Engineering, 2324 Main Mall. Fellow AIAA.
‡Professor, System Engineering, 3-1-1 Yoshinodai.

experimental results is also performed to validate the model and to assess contributions of various physical as well as geometrical parameters to the time constant of nutational divergence.

II. Ground-Based Experiment

The configuration of the ground-based experiment is schematically shown in Fig. 1. The experiment was performed in the space chamber at the Noshiro Testing Center of ISAS. The spacecraft model, with two spherical tanks containing glycerin or water, was supported by a gas (He) bearing and spun at a desired speed by an electric motor. Attitude motion of the model was constrained by other mechanical bearings at the bottom during the spin-up phase. On reaching the target spin rate ω_{sp}, the motor, as well as the mechanical bearings, was removed, and the model began free motion. The attitude time histories of various configurations were recorded using a visual sensor for 10–15 min for each case. The corresponding nutational time constants were then calculated through the least-squares method using the data after the major transient effects had died down.

III. System Modeling

A mathematical model is also developed for dynamical simulation of the system. The model consists of three rigid bodies, as shown in Fig. 2. Bodies 2 and 3, representing the liquid fuel, are connected to body 1 (the third stage) by spherical joints located at the centers of the spherical tanks. Body 1 is supported by the ground through a spherical joint, which corresponds to the gas bearing. Generalized coordinates for the system are the following Euler angles (Fig. 3): ϕ, ψ, and λ for the main body and q_{ix}, q_{iy}, and q_{iz} for the liquid ($i = 2, 3$). Their orders of rotation are $\lambda \rightarrow \psi \rightarrow \phi$ and $q_{iz} \rightarrow q_{iy} \rightarrow q_{ix}$, respectively.

The mass, inertia matrix, and c.m. offset of the liquid can be obtained as

$$m_i = (\pi/3)\rho_i H_i^2(3R_i - H_i) \tag{1a}$$

$$I_i = \begin{bmatrix} I_a & 0 & 0 \\ 0 & I_a & 0 \\ 0 & 0 & I_b \end{bmatrix} \tag{1b}$$

$$\boldsymbol{b}_i = \{0, 0, l_z\}^T \qquad (i = 2, 3) \tag{1c}$$

where ρ_i, R_i, and H_i are the density, radius, and height of the liquid, respectively, and

$$I_a = (\pi\rho_i/60)\left[z\left(15R_i^4 + 10R_i^2z^2 - 9z^4\right)\right]_{z=-R_i}^{-R_i+H_i} \tag{1d}$$

$$I_b = (\pi\rho_i/30)\left[z\left(15R_i^4 - 10R_i^2z^2 + 3z^4\right)\right]_{z=-R_i}^{-R_i+H_i} \tag{1e}$$

$$l_z = \frac{3(2R_i - H_i)^2}{4(3R_i - H_i)} \tag{1f}$$

Physical and geometrical parameters for the nominal configuration are listed in Table 1.

A. Liquid Friction Model

Liquid friction is introduced as a generalized force. To obtain the friction force and torque, a liquid-fixed frame (L-frame), with the

Table 1 Physical and geometrical parameters of the nominal M-3SII model

Third stage (body 1)	Liquid (body i, $i = 2, 3$)
$m_1 = 61.4$ kg	$R_i = 0.0975$ m
$(I_{xx})_1 = 7.89$ kgm^2	$H_i = 0.0975$ m
$(I_{yy})_1 = 7.89$ kgm^2	$\rho_i = 1.264 \times 10^3$ kg/m^3
$(I_{zz})_1 = 4.99$ kgm^2	(glycerin, 20°C)
$(I_{xy})_1 = (I_{yz})_1 = (I_{zx})_1 = 0$	$= 0.998 \times 10^3$ kg/m^3
	(water, 20°C)
Geometrical parameters	
$\boldsymbol{b}_1 = \{0, 0, 0\}^T$ m	
$\boldsymbol{a}_2 = \{0, -0.155, 0.145\}^T$ m	
$\boldsymbol{a}_3 = \{0, 0.155, 0.145\}^T$ m	

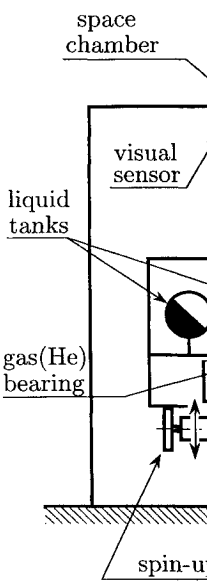

Fig. 1 Ground-based experimental setup for nutation analysis of the spinning satellite.

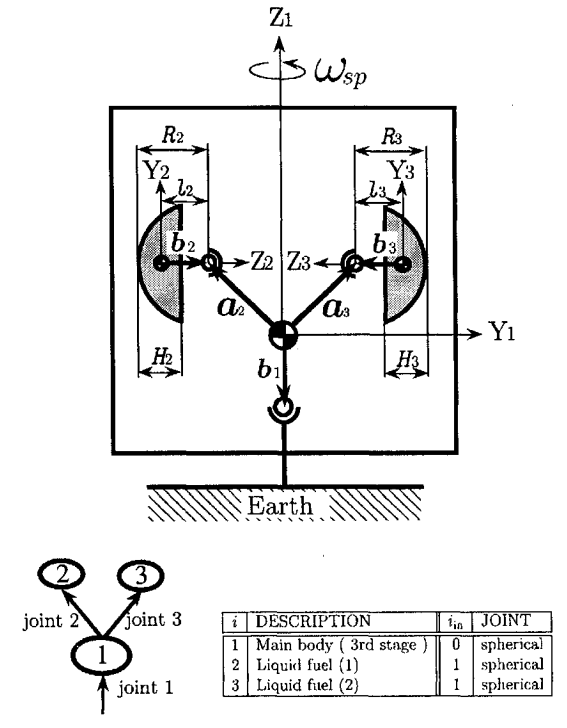

Fig. 2 Mathematical model for the ground-based experiment.

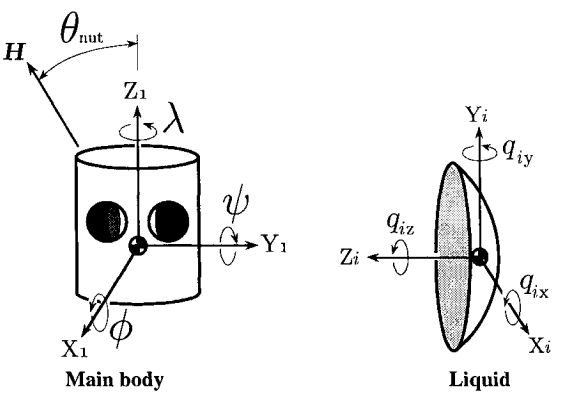

Fig. 3 Generalized coordinates for the spacecraft model.

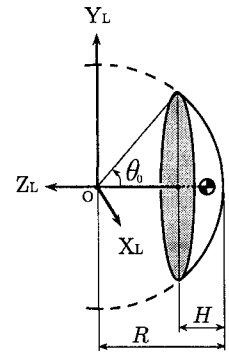

Fig. 4 Liquid-fixed coordinate (L-frame).

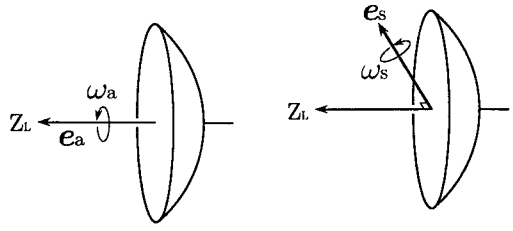

Fig. 5 Two modes of liquid motion in a spherical tank.

origin located at the tank center and the axes parallel to X_i, Y_i, and Z_i ($i = 2$ or 3) is used (Fig. 4). The position vector to an arbitrary point on the spherical surface of the liquid with respect to the L-frame can be expressed as

$$\boldsymbol{r} = R\boldsymbol{e}_r \tag{2}$$

where $\boldsymbol{e}_r$ is the unit vector of the radial direction. Let ω denote the angular velocity vector of the L-frame with respect to the main body-fixed frame. Then the velocity of the point relative to the main body (L-frame expression) can be written as

$$\boldsymbol{v} = [\boldsymbol{\omega}\times]\boldsymbol{r} = R[\boldsymbol{\omega}\times]\boldsymbol{e}_r \tag{3}$$

where $[\boldsymbol{a}\times]$ is a 3×3 matrix equivalent to the vector product operation $\boldsymbol{a}\times$, defined as

$$[\boldsymbol{a}\times] \equiv \begin{bmatrix} 0 & -a_3 & a_2 \\ a_3 & 0 & -a_1 \\ -a_2 & a_1 & 0 \end{bmatrix} \tag{4}$$

Noting that the liquid is symmetrically distributed about the Z_L axis, its motion can be divided into two modes: rotation around the Z_L axis and that around an axis normal to the Z_L axis (Fig. 5). They are often referred to as agitation and sloshing, respectively. Based on the preceding considerations, the angular velocity ω is also divided as

$$\boldsymbol{\omega} = \omega_a\boldsymbol{e}_a + \omega_s\boldsymbol{e}_s \tag{5a}$$

where ω_a and ω_s are the contributions of agitation and sloshing to the angular velocity, respectively, defined as

$$\omega_a = |\omega_z|, \qquad \omega_s = \sqrt{\omega_x^2 + \omega_y^2} \tag{5b}$$

and $\boldsymbol{e}_a$ and $\boldsymbol{e}_s$ are unit vectors representing agitation and sloshing axes, respectively, i.e.,

$$\boldsymbol{e}_a = \{0, 0, \text{sign}(\omega_z)\}^T, \qquad \boldsymbol{e}_s = \{\omega_x/\omega_s, \omega_y/\omega_s, 0\}^T \tag{5c}$$

Substituting for ω from Eq. (5a) into Eq. (3), relative velocity can be expressed in terms of the contributions of the two modes as

$$\boldsymbol{v} = V_a\boldsymbol{v}_a + V_s\boldsymbol{v}_s \tag{6a}$$

where

$$V_m = R\omega_m, \qquad \boldsymbol{v}_m = [\boldsymbol{e}_m\times]\boldsymbol{e}_r \qquad (m = a, s) \tag{6b}$$

Here it is assumed that, for each mode, the resulting friction force is proportional globally to $(V_m)^{N_m}$ and locally to $\boldsymbol{v}_m$ ($m = a, s$). Thus, the frictional force acting on an infinitesimal contacting area dS can be written as

$$d\boldsymbol{f}_L = -\left\{C_a(V_a)^{N_a}\boldsymbol{v}_a + C_s(V_s)^{N_s}\boldsymbol{v}_s\right\} dS \tag{7}$$

where C_a, C_s, N_a, and N_s are all constants. Total friction force and torque (with respect to the L-frame) are

$$\boldsymbol{f}_L = \int_S d\boldsymbol{f}_L, \qquad \boldsymbol{\tau}_L = \int_S [\boldsymbol{r}\times]\, d\boldsymbol{f}_L \tag{8}$$

where S denotes the contacting surface. Substituting from Eqs. (2), (6b), and (7) into Eq. (8) and integrating over S yield

$$\boldsymbol{f}_L = F_s(\omega)c(H)[\boldsymbol{e}_s\times]\boldsymbol{e}_a \tag{9a}$$

$$\boldsymbol{\tau}_L = R\{F_s(\omega)s(H)\boldsymbol{e}_s + F_a(\omega)a(H)\boldsymbol{e}_a\} \tag{9b}$$

where H is the height of the liquid (Fig. 4) and

$$F_m(\omega) \equiv \pi R^2 C_m (V_m)^{N_m} \qquad (m = a, s) \tag{10a}$$

$$c(H) \equiv 1 - (\cos\theta_0)^2 \tag{10b}$$

$$s(H) \equiv (\cos\theta_0)^3 + \cos\theta_0 - 1 \tag{10c}$$

$$a(H) \equiv 2\{-(\cos\theta_0)^3 + \cos\theta_0 - 1\} \tag{10d}$$

$$\cos\theta_0 \equiv (R - H)/R \tag{10e}$$

For application, nondimensionalization of Eq. (9) would be useful. Here the reference value used for the force is

$$F_0 \equiv mR\omega_{sp}^2 \tag{11}$$

Using this value for F_0, Eq. (10a) is nondimensionalized as

$$F_m/F_0 = C_m^*(\omega_m/\omega_{sp})^{N_m} \qquad (m = a, s) \tag{12a}$$

where

$$C_m^* \equiv \frac{F_m|_{\omega_m = \omega_{sp}}}{F_0} = \frac{\pi R^2 C_m (R\omega_{sp})^{N_m}}{F_0} \qquad (m = a, s) \tag{12b}$$

Nondimensional constants C_a^*, C_s^*, N_a, and N_s are used as liquid friction model parameters hereafter.

B. System Equations of Motion

Since the inertia parameters and the friction are now identified, the system equations of motion are derived using the procedures of Refs. 8 and 9. The dynamics of the body i ($i = 1, 2, 3$) can be described as

$$\boldsymbol{M}_i\dot{\boldsymbol{u}}_i = \boldsymbol{G}_i \tag{13}$$

where $\boldsymbol{u}_i$ is the generalized velocity consisting of the translational and angular velocity vectors of the local frame fixed to the body i at its c.m. $\boldsymbol{M}_i$ and $\boldsymbol{G}_i$ are the mass matrix and the total force, respectively. The latter includes the friction, gravity, and the gyroscopic moments. The body i is preceded by a body with the number $i_{\text{in}}(i)$, which is referred to as the inboard body (Fig. 2). The generalized velocity and acceleration of the body i can be expressed recursively as

$$\boldsymbol{u}_i = \boldsymbol{P}_i^u\boldsymbol{u}_{i_{\text{in}}} + \boldsymbol{P}_i^c\boldsymbol{u}_i^c + \boldsymbol{p}_i^{\text{cu}} \tag{14a}$$

$$\dot{\boldsymbol{u}}_i = \boldsymbol{P}_i^u\dot{\boldsymbol{u}}_{i_{\text{in}}} + \boldsymbol{P}_i^c\dot{\boldsymbol{u}}_i^c + \boldsymbol{p}_i^c \tag{14b}$$

where $\boldsymbol{u}_i^c$ is the angular velocity of the spherical joint i. Detailed descriptions of the matrices $\boldsymbol{P}_i^u$, $\boldsymbol{P}_i^c$, $\boldsymbol{p}_i^{\text{cu}}$, and $\boldsymbol{p}_i^c$, representing the joint constraint, appear in Ref. 8. Equations (13) and (14b) yield the system equation of motion as

$$\boldsymbol{M}^c\dot{\boldsymbol{u}}^c = \boldsymbol{G}^c \tag{15}$$

where

$$\boldsymbol{M}^c = [(\boldsymbol{E} - \boldsymbol{P}^u)^{-1}\boldsymbol{P}^c]^T \boldsymbol{M}[(\boldsymbol{E} - \boldsymbol{P}^u)^{-1}\boldsymbol{P}^c] \tag{16a}$$

$$\boldsymbol{G}^c = [(\boldsymbol{E} - \boldsymbol{P}^u)^{-1}\boldsymbol{P}^c]^T \{\boldsymbol{G} - \boldsymbol{M}(\boldsymbol{E} - \boldsymbol{P}^u)^{-1}\boldsymbol{p}^c\} \tag{16b}$$

$$(\boldsymbol{P}^u)_{(i,j)} = \delta_{i_{\text{in}}(i),j}\boldsymbol{P}_i^u, \qquad (\boldsymbol{P}^c)_{(i,j)} = \delta_{i,j}\boldsymbol{P}_i^c \tag{16c}$$

$$\boldsymbol{M} = \text{diag}[\ldots, \boldsymbol{M}_i, \ldots], \qquad \boldsymbol{G} = \{\ldots, \boldsymbol{G}_i^T, \ldots\}^T \tag{16d}$$

Here $\boldsymbol{E}$ is the unit matrix, the left-hand sides of Eq. (16c) denote the (i, j)-block elements, and $\delta_{i,j}$ is the Kronecker delta.

C. Nutation Angle and Its Time Constant

For interpretation of attitude dynamics of systems with energy dissipation, nutation angle θ_{nut} and its time constant T_{nut} are often used. The former is defined as the angle between the system angular momentum vector and the spin axis (Fig. 3), i.e.,

$$\theta_{\text{nut}} = \arccos(\boldsymbol{e}_h^T \boldsymbol{e}_{z1}) \tag{17}$$

where $\boldsymbol{e}_h$ and $\boldsymbol{e}_{z1}$ are unit vectors parallel to the system angular momentum vector and the spin axis (the main body-fixed Z_1 axis), respectively. The nutation angle θ_{nut} diverges when the system has energy dissipation, and so it is often valid to approximate its time history using the exponential function as

$$\theta_{\text{nut}}(t) \approx C \exp(t/T_{\text{nut}}) \tag{18}$$

to appreciate the average motion. In the equation, C and T_{nut} are constants dependent on the parameters and initial conditions of the system. They are determined from the response obtained through the least-squares method. To guarantee their accuracy, simulation time is selected so that half the data also give almost identical value of T_{nut}. Usually, the nutational time constant is insensitive to initial conditions for a given system. For instance, simulation of a system with a typical set of parameters, $C_a^* = C_s^* = 0.55 \times 10^{-2}$ and $N_a = N_s = 1.0$, undergoing the initial nutation angle of $\theta_{\text{nut}}(0) = 2$ deg results in the best fitting time constant of 337.3 s, whereas a completely different disturbance of $\theta_{\text{nut}}(0) = 0.1$ deg also gives nearly the same value of $T_{\text{nut}} = 336.9$ s, though the details of the responses are quite different. Therefore the nutation time constant T_{nut} is considered to be a good macroscopic parameter for description of nutational characteristics of the system. In the ground-based experiment, motion of the liquid, as well as initial conditions (disturbances), was unknown, and so a direct comparison of the responses based on the experiment and the numerical simulation could not be made. Hence, in the following sections, T_{nut} is used as the criterion for correspondence between the experimental and numerical results.

IV. Parametric Study

Based on the given modeling, a parametric response study was carried out. Numerical data were obtained using the general multibody simulation program described in Refs. 8 and 9.

A. Nominal Model Parameters

Figure 6 shows response of the system model with the model parameters as $C_a^* = C_s^* = 0.55 \times 10^{-2}$ and $N_a = N_s = 1.0$. The spin rate ω_{sp} is 2 rps. As mentioned before, the nutation time constant has turned out to be quite insensitive to the initial nutation angle and, hence, it is selected arbitrarily as 0.1 deg. Equilibrium configuration of the liquid with reference to the main body is governed by the centrifugal, gravitational, and gyroscopic moment balance

$$q_{ix} = -18.11 \text{ deg}, \qquad q_{iy} = q_{iz} = 0 \text{ deg} \qquad (i = 2, 3)$$

Time history of the spin angle λ is almost linear ($\lambda \approx \omega_{\text{sp}} t$). Nutation excites relative motion between the main body and the liquid, which results in energy dissipation, and the nutational response diverges. Figure 6a shows that the exponential function in Eq. (18) fits the time history of θ_{nut} well. The best fitting parameters, obtained through the least-squares method, are $C = 0.102$ deg and $T_{\text{nut}} = 309.9$ s.

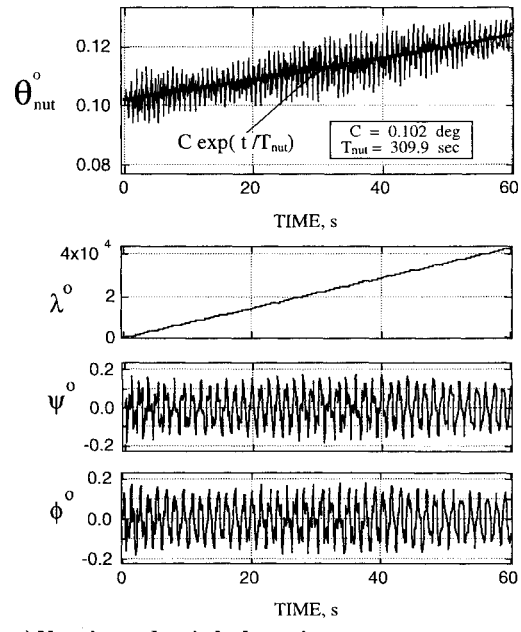

a) Nutation and main body motions

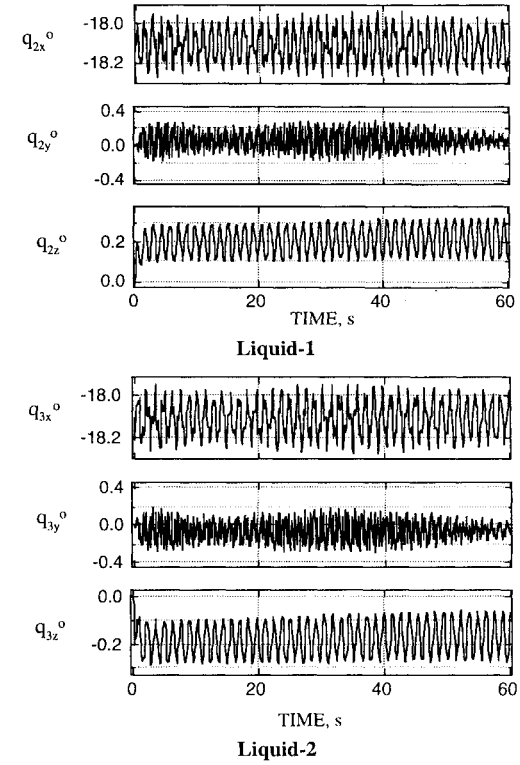

b) Liquid motions

Fig. 6 Response of the ground-based model with the nominal friction parameters.

The experiment also gave the time constant of about 300 s for the nominal configuration with glycerin as liquid. Hence, this case will be referred to as the nominal. Liquid motions of the same case are shown in Fig. 6b, where, as defined in Fig. 3, q_{ix}, q_{iy}, and q_{iz} denote the vertical slosh, horizontal slosh, and agitation angles of the liquid i ($i = 2, 3$), respectively. With the initial nutation angle as disturbance, the liquid masses begin relative motions. Basic frequency of the vertical slosh and the agitation is 0.75 Hz. Slosh with a higher frequency is also induced especially in the horizontal direction (q_{2y} and q_{3y}). This is considered to be due to the constraint force through the bearing support, as will be discussed later. The physical property of water is closer to that of the actual fuel, but, because of its low viscosity, results of the ground-based experiment with water have relatively larger variance with values of the time constant in the range

of 1050–1120 s. Simulation results gave $T_{nut} = 1016$ s for the liquid model parameters $C_a^* = C_s^* = 2.0 \times 10^{-3}$ and $N_a = N_s = 1.0$.

B. Scale Effect

Consideration of scale effect is necessary for interpretation of the experimental data. Here influence of the offset and size of the tanks is assessed. Simulation with the nominal liquid parameters and tanks located 45 mm inside of the nominal configuration gave the time constant of 255.4 s. It is 18% smaller than that of the results for the nominal case (Fig. 6). The reduction in the time constant was also observed in the experiment with its value of $T_{nut} = 190$–230 s. Numerical result indicates that the time constant increases to 1072.8 s for the model with the nominal liquid parameters and smaller tanks ($R = 7.25$ cm). This is because the total friction decreases due to a reduction in the contact area between the tanks and the liquid. The experimental value of $T_{nut} \approx 1600$ s shows a disparity because of the slow divergence of the nutation angle. Still the results suggest that the mathematical model can account for the general trend of the experimental data.

C. Correspondence with the System in Space

In the ground tests, the spacecraft model was supported by the gas bearing at a point that is geometrically fixed to the main body. The point does not coincide with the system c.m. This represents the most significant discrepancy. Its effect can be investigated by the numerical simulation of a model in space with the same system parameters as those of the ground test. This can be achieved through replacing the joint 1 in Fig. 2 (spherical joint) with a free joint and dropping the gravitational terms. Figure 7 shows the response of the system with the nominal configuration in free space. The time constant of 416.3 s is 34% larger than that of the corresponding simulation results for the ground configuration (Fig. 6). Simulation of the system in space with smaller tanks gave the time constant of 1482 s, which is 38% above the values for the ground configuration. This implies that, in general, the ground-based experiments can give smaller values for the time constant, suggesting faster divergence of the nutational response and larger dissipation of energy. The bearing support imparts an extra constraint force between the main body and the Earth, which indirectly excites the relative motion and, hence, the friction between the main body and the liquid. This is confirmed by the high-frequency slosh observed in Fig. 6b that is not present in space (Fig. 7b). Despite the highly nonlinear and coupled dynamics with energy dissipation, the free space cases keep the angular momentum almost constant (with less than 5×10^{-9}% of error), supporting validity of the formulation, as well as computational accuracy of the program.

D. Effect of the Main Body C.M. Offset

It has been shown that the bearing support affects the time constant of the nutational divergence. In the experiment, the spacecraft model is dynamically balanced around its spin axis, with which the main body c.m. is aligned well. However, the gas bearing is slightly offset vertically from the c.m., and this can lead to discrepancy in the response and the associated time constant. Simulations are carried out for cases where the main body's c.m. is taken to be 2 cm above and below the bearing support. They give the nutation time constant values of 277.6 and 346.0 s, respectively, whereas that for the nominal case (Fig. 6) was 309.9 s. These results are understandable because a higher location of the c.m. destabilizes the system, like an inverted pendulum, whereas a lower c.m. stabilizes it. Correspondingly, the relative motion of the liquid with respect to the main body varies.

V. Theoretical Estimation of the Liquid Parameters

To appreciate the preceding results physically, the liquid friction model parameters are also estimated using the laminar plate flow theory. Consider an infinite plate oscillating in liquid with density and kinematic viscosity as ρ and ν, respectively. Let the relative velocity of the plate with respect to the liquid be

$$\boldsymbol{u} = \boldsymbol{u}_0 \cos(\omega_p t) \tag{19}$$

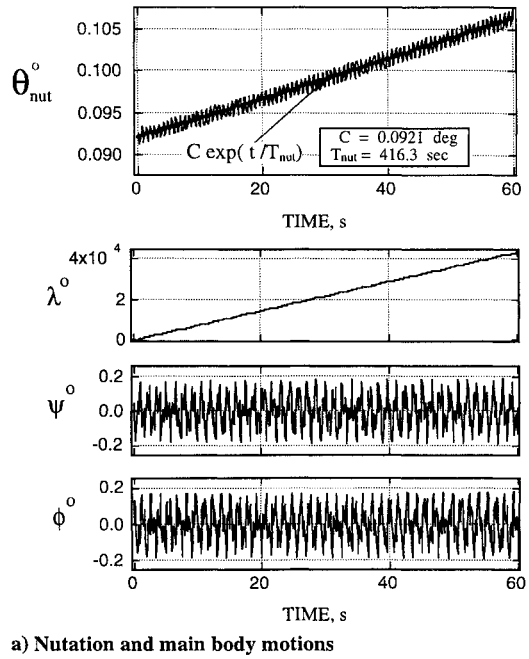

a) Nutation and main body motions

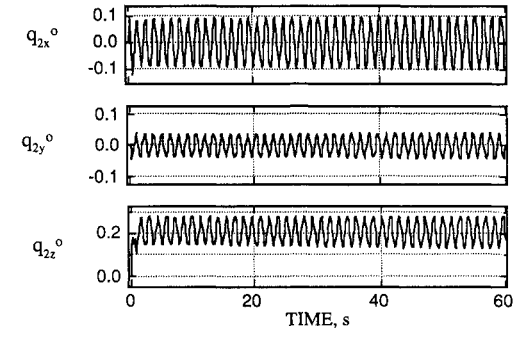

Liquid 1

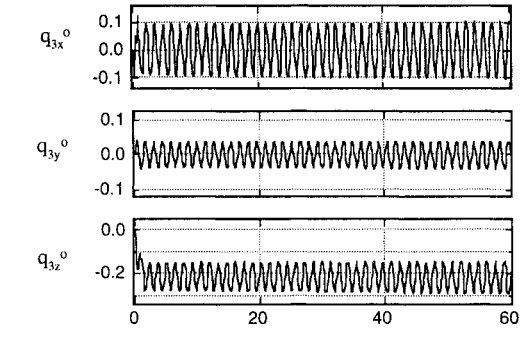

Liquid 2

b) Liquid motions

Fig. 7 Response of the nominal model in free space.

Then the shearing force acting on an infinitesimal plate element area $\mathrm{d}S$ can be written as[10]

$$\mathrm{d}\boldsymbol{f}_L = -\rho(\omega_p \nu)^{\frac{1}{2}} \boldsymbol{u}_0 \cos(\omega_p t + \pi/4)\, \mathrm{d}S \tag{20a}$$

Neglecting the phase difference between Eqs. (19) and (20a),

$$\mathrm{d}\boldsymbol{f}_L = -\rho(\omega_p \nu)^{\frac{1}{2}} \boldsymbol{u}\, \mathrm{d}S \tag{20b}$$

Noting Eq. (6a), Eq. (20b) corresponds to Eq. (7) with parameters

$$N_m = 1, \qquad C_m = \rho(\omega_{p,m} \nu)^{\frac{1}{2}} \qquad (m = a, s) \tag{21}$$

where $\omega_{p,a}$ and $\omega_{p,s}$ are agitation and sloshing frequencies, respectively. Hence, the proposed friction model is a natural extension of the plate flow model through consideration of the overall effect

Table 2 Comparison of the nutation time constants obtained experimentally and numerically

Case	$T_{nut}/(T_{nut})_{nominal}$ Numerical	Experimental
Tanks, 45 mm inside	0.82	0.70
Smaller tanks ($R = 9.75 \rightarrow 7.25$ cm)	3.46	5.20
Faster spin ($\omega_{sp} = 2 \rightarrow 3$ rps)	0.92	0.90

due to the wall curvature, finite contacting area, etc., by modifying the parameter C_m. Substitution from Eqs. (21), (1a), and (11) into Eq. (12b) gives the dimensionless parameter C_m^* as

$$C_m^* = 3\left(\frac{H}{R}\right)^{-2}\left(3-\frac{H}{R}\right)^{-1}\frac{(\omega_{p,m}\nu)^{\frac{1}{2}}}{R\omega_{sp}} \qquad (m=a,s) \quad (22)$$

For the nominal cases during the simulation, values related to the liquid are

$$R = H = 0.0975\,\text{m}, \qquad \omega_{sp} = 2.00\,\text{rps} = 12.57\,\text{rad/s}$$
$$\omega_{p,m} \approx 0.75\,\text{Hz} = 4.71\,\text{rad/s} \qquad (m=a,s) \quad (23)$$
$$(\nu,\rho) = \begin{cases} (7.48\times10^{-4},\ 1.26\times10^{3}) & \text{for glycerine} \\ (1.00\times10^{-6},\ 1.00\times10^{3}) & \text{for water} \\ (1.28\times10^{-6},\ 1.03\times10^{3}) & \text{for hydrazine} \end{cases}$$
$$(\text{m}^2/\text{g},\ \text{kg/m}^3)$$

which lead to

$$C_m^* = \begin{cases} 7.24\times10^{-2} & \text{for glycerine} \\ 2.65\times10^{-3} & \text{for water} \\ 3.00\times10^{-3} & \text{for hydrazine} \end{cases} \qquad (m=a,s) \quad (24)$$

The corresponding model parameters obtained through numerical simulation in conjunction with the experimental data were $C_m^* = 5.5\times10^{-3}$(glycerine) and 2.0×10^{-3}(water). Comparison of these values indicates that, in general, the plate flow theory tends to overestimate the liquid friction parameters; however, the discrepancy is relatively small for water. A large error for glycerine may be attributed to the laminar flow assumption [Eq. (20a)]. Because the major objective of this paper is extrapolation of the ground-based experimental data to space systems, the liquid oscillation frequency $\omega_{p,m}$ in Eq. (23) is obtained through the numerical analysis in Sec. IV.A, which is in good correspondence with the experimental results. To estimate $\omega_{p,m}$ without experiment, one may assume its certain value and correct it through numerical simulation until sufficient convergence is attained.

Equation (22) helps to estimate the liquid model parameters for different systems. Assuming $\omega_{p,m} \propto \omega_{sp}$ for a given geometrical configuration, Eq. (22) gives

$$C_m^* \propto \omega_{sp}^{-\frac{1}{2}} \quad (25)$$

Equation (25) yields $C_m^* = 1.63\times10^{-3}$ for a system with the same geometry as the nominal case for water and a faster spin rate (3 rps). The numerical simulation using this parameter value leads to the nutation time constant of 936.5 s, which corresponds to 92% of that for the nominal spin rate (1016 s). In the experiment, an increase in the spin rate from 2 to 3 rps resulted in the time constant of 960–998 s, which represents around 90% of the nominal value for water as liquid (1050–1120 s). A comparison of the numerical and experimental results supports the validity of Eq. (25) for a given configuration. The equilibrium orientation of the liquid changes to $q_{2x} = q_{3x} = -8.2$ deg from the values for the nominal spin rate (-18.1 deg) due to an increase in the centrifugal force by the spin.

Finally, comparison of the nutation time constants obtained using the experimental and numerical approaches is summarized in Table 2. Despite the simple liquid friction model, the results show rather good correspondence. This supports validity of the rigid-tree formulation as well as the liquid friction model [Eq. (9)], implying the importance of the multibody dynamics aspect of the problem. The relatively large discrepancy for the case with smaller tanks may be attributed to the difficulty in measuring the very slow nutational divergence, yielding increased errors in the experimental values.

VI. Concluding Remarks

Multibody interaction between spin-stabilized satellites and their liquid fuel sloshing, as well as its effect on the nutation time constant, has been investigated based on a rigid-tree model. The liquid has finite inertia and three degrees of freedom representing longitudinal and lateral sloshes, as well as circulatory motion about its axis of symmetry. A liquid friction model is proposed and introduced to the nonlinear equations of motion as a generalized force. The liquid friction parameters are evaluated both experimentally and theoretically, though the latter tends to overestimate the liquid friction parameters. The simulation results compare rather well with the experimental values, suggesting the importance of the multibody dynamics aspect of the problem. The numerical study also indicates that ground-based experiments can underestimate the nutation time constants of the corresponding systems in space. This is mainly due to the extra constraint force introduced by the bearing support, exciting the relative motions indirectly. The successful prediction of the trends of the nutation time constants is encouraging although the model should be modified to consider the internal liquid motions to obtain higher accuracy, especially for large tanks where the internal energy dissipation dominates the boundary-layer friction.

Acknowledgments

The authors are indebted to J. Kawaguchi and S. Sawai of the Institute of Space and Astronautical Science (ISAS, Japan) for providing them with the ground-based experimental data of the M-3SII model. The mainframe computer of ISAS was used to obtain the numerical data.

References

[1]Miles, J. W., and Troesch, B. A., "Surface Oscillations of a Rotating Liquid," *Journal of Applied Mechanics*, Vol. 28, No. 4, 1961, pp. 491–496.

[2]Hwang, C., "Longitudinal Sloshing of Liquid in a Flexible Hemispherical Tank," *Journal of Applied Mechanics*, Vol. 32, No. 3, 1965, pp. 665–670.

[3]Wolf, J. A., Jr., "Whirl Dynamics of a Rotor Partially Filled with Liquid," *Journal of Applied Mechanics*, Vol. 35, No. 4, 1968, pp. 676–682.

[4]Hendricks, S. L., and Morton, J. B., "Stability of a Rotor Partially Filled with a Viscous Incompressible Fluid," *Journal of Applied Mechanics*, Vol. 46, Dec. 1979, pp. 913–918.

[5]El-Raheb, M., and Wagner, P., "Vibration of a Liquid with a Free Surface in a Spinning Spherical Tank," *Journal of Sound and Vibration*, Vol. 76, No. 1, 1981, pp. 83–93.

[6]Slafer, L. I., and Challoner, A. D., "Propellant Interaction with the Payload Control System of Dual-Spin Spacecraft," *Journal of Guidance, Control, and Dynamics*, Vol. 11, No. 4, 1988, pp. 343–351.

[7]Agrawal, B. N., "Dynamic Characteristics of Liquid Motion in Partially Filled Tanks of a Spinning Spacecraft," *Journal of Guidance, Control, and Dynamics*, Vol. 16, No. 4, 1993, pp. 636–640.

[8]Nagata, T., "Dynamics of Flexible Multibody Systems: A Formulation with Applications," Ph.D. Thesis, Dept. of Aerospace Engineering, Univ. of Tokyo, Tokyo, Japan, March 1995.

[9]Nagata, T., Modi, V. J., and Matsuo, H., "An Approach to Dynamics and Control of Flexible Systems," AIAA Paper 94-3756, Aug. 1994.

[10]Komatsu, K., and Shimazu, J., "Theoretical Estimation of the Viscous Damping from Liquid Transient Motion in Tanks," National Aerospace Lab., TR 1095, Tokyo, Japan, Feb. 1991 (in Japanese).